Compaction of noncohesive and cohesive granular materials under vibrations: Experiments and stochastic model

J.-E. Mathonnet and P. Sornay
CEA, DEN, DEC, SFER, LCU, 13108 Saint-Paul-Lez-Durance, France

M. Nicolas and B. Dalloz-Dubrujeaud
Aix Marseille Univ, CNRS, IUSTI, Marseille, France

(Received 24 May 2016; revised manuscript received 8 November 2016; published 28 April 2017)

We study the time evolution of the compaction of a noncohesive or cohesive granular material submitted to shaking through experiments and a stochastic model. Beyond well-known empirical expressions, we show that the characteristic time scales depend on the number of objects in the assembly. For a noncohesive granular material, the compaction time scale is governed by the number of individual grains in the system. In the case of a cohesive granular material, a two-scale model (individual particles and clusters) allows one to mimic the time evolution of the compaction of an actual cohesive powder driven by horizontal vibrations. In this case, the two time scales are associated with the numbers of clusters and grains, respectively.

DOI: 10.1103/PhysRevE.95.042904

I. INTRODUCTION

Ubiquitous in many natural and industrial processes, granular matter provides many challenges when it needs to be stored or transported. An external mechanical energy is often needed to allow motion or to compact an initially loose packing. This is especially true when the grains exhibit some cohesive properties, however, cohesive powders are very common in many industries (pharmaceutical powders, flours, cements, nuclear powders, among other examples).

For at least two decades, numerous studies have focused on the compaction and the density relaxation of a granular assembly submitted to shaking. Among them, the works on density relaxation by vertical tapping lead to empirical laws based on an inverse logarithmic law [1,2] for the particle volume fraction

$$\phi(t) = \phi_\infty - \frac{\phi_\infty - \phi_0}{1 + B\ln(1 + t/\tau)}, \tag{1}$$

or on a stretched exponential [3] derived from a Kohlrausch-Williams-Watts (KWW) model

$$\phi = \phi_\infty - (\phi_\infty - \phi_0)e^{-(t/\tau)^\beta}. \tag{2}$$

Both laws exhibit an initial value ϕ_0, a limit value ϕ_∞, a characteristic time τ, and some fitting parameters B or β.

These studies considered a set of spherical granular particles of the same size without surface forces between them (i.e., noncohesive particles). When the granular system exhibits cohesive properties, some new difficulties arise during industrial or natural processes. A cohesive powder usually exhibits a very large angle of repose and a weak flowability. The flowability of a powder is often characterized by the Hausner index (I_H) [4], which is the ratio of the tapped bulk density of the powder over the freely settled bulk density. A Hausner ratio of greater than 1.25 is considered to be an indication of poor flowability. The filling and emptying of a silo are difficult without an external input of energy, often mechanical, and the packing of grains may have a very small bulk density due to the presence of macrocavities, bulk holes, and vaults. A two-dimensional (2D) numerical system of cohesive grains has been studied by Gilabert *et al.* [5,6], with a focus on static packings and plastic consolidation. More recently, three-dimensional (3D) numerical simulations showed the effects of nonconvexity on the packing fraction [7]. The flow of cohesive powders has also been studied numerically [8], but the vibration-induced compaction of cohesive powders is a recent subject [9] and many aspects still need to be explored.

In this paper we aim to investigate the long-time density evolution of a bed of noncohesive and cohesive granular material under vibrations, through experiments on three sets of particles and also through a stochastic model.

II. EXPERIMENTS

We first benchmarked our experimental setup with a noncohesive granular material, by performing compaction experiments on a set of glass beads of $d = 130\ \mu$m mean diameter with $I_H = 1.08$. The container was a 15×15 mm^2 square section tank with a height of 25 cm. This container was horizontally shaken at 100 Hz with a $3g$ acceleration by an electromagnetic shaker. Experiments with various quantities of beads (hence different initial heights H_0) were performed. Great care was taken during the filling process to ensure that the initial packing fraction was constant for each experiment. Through the measurement of the packing height $H(t)$, we have recorded the particle volume fraction $\phi(t)$, where the time t is the number of vibration cycles from the start.

Figure 1 shows the compaction data $\phi(t)$ for five different initial heights H_0 of glass bead packings in a semilog scale. The packing fraction starts at ϕ_0, shows an increase at $t \approx 10^2$, and then saturates at a ϕ_∞ value near $t \approx 10^3$. These experimental data are reasonably well fitted by the stretched exponential function [Eq. (2)] with $\beta = 1$. The dependence of the final packing on the size of the box and/or the height of the packing has already been observed in 2D trough numerical simulations [10] and was not further investigated in our work.

The compaction behavior is quite different when the granular material exhibits a cohesive property. We measured

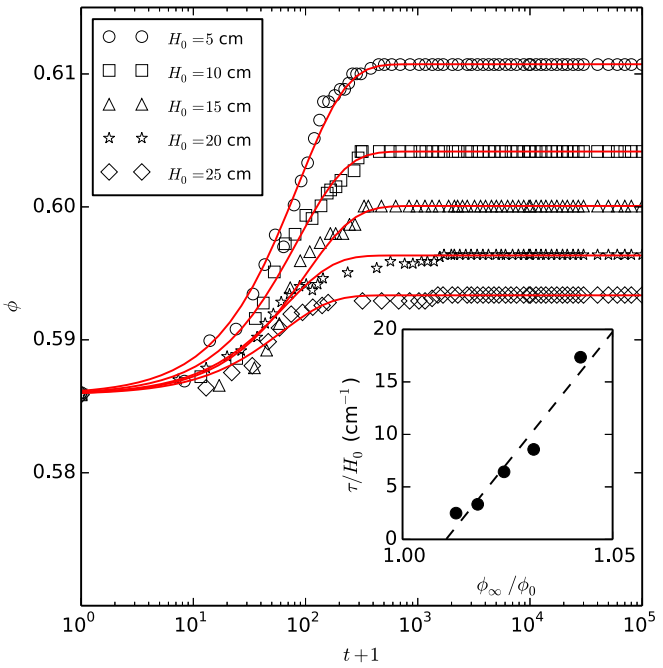

FIG. 1. Experimental compaction on glass beads with various initial heights (hence masses) of the beads. The data are fitted with $\beta = 1$ in Eq. (2). Inset: Characteristic compaction time τ/H_0 vs ϕ_∞/ϕ_0 for glass bead experiments.

experimentally the compaction process for a cohesive powder. The powder was a polydisperse UO_2 powder with a mean diameter $d = 30\ \mu$m, and the grain surfaces were very rough (Fig. 2) due to the granulation process. The cohesive property ($I_H = 1.53$) comes from this surface roughness and we checked that the cohesion was not due to humidity or triboelectric effects. The powder was held in the same vertical parallelepiped tank. The tank was vibrated horizontally with an electromagnetic shaker with a frequency range of 30–100 Hz, and a normalized acceleration of $3g$–$9g$. The packing of this assembly of grains obviously presented large-scale voids, vaults, or macrocavities. This can be observed in Fig. 3 for a vibrated cohesive powder where large-size voids are present

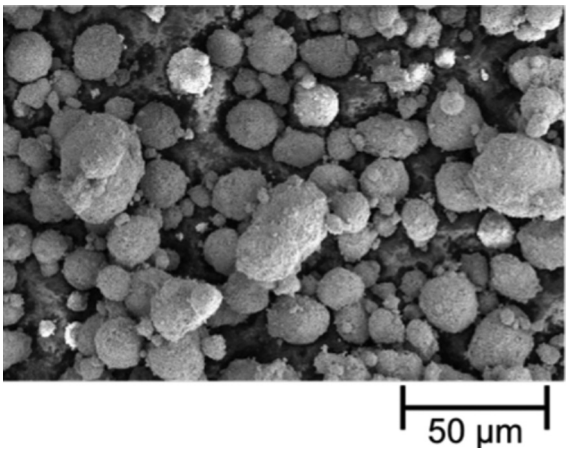

FIG. 2. Scanned electronic microscope image of the UO_2 cohesive powder.

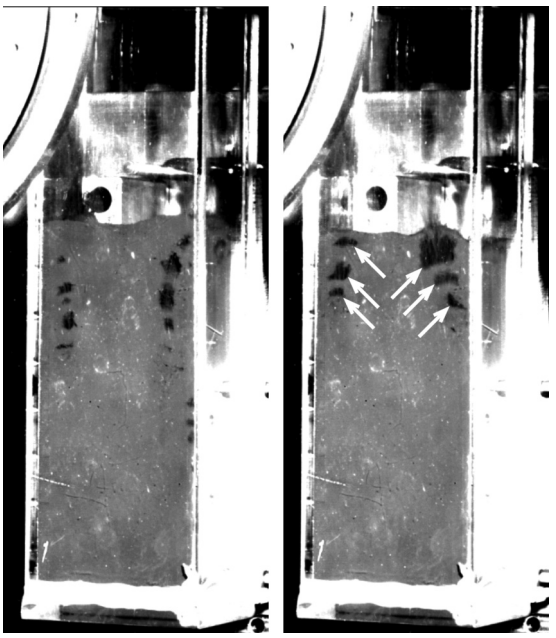

FIG. 3. Observation of macrocavities (highlighted by white arrows) in a vibrated cohesive UO_2 powder. $t = 936$ cycles (left) and $t = 1254$ cycles (right).

near the tank wall. Numerous other macrocavities are assumed to exist in the bulk of the powder.

A representative experimental result of the compaction process is shown in Fig. 4 for different initial heights of the powder, vibrated at 100 Hz with a $7g$ acceleration. The packing fraction increases at a short time (a few thousands cycles), reaches a plateau for $t \approx 10^4$, and then a second long-time increase occurs, much more slowly. A two-stage compaction is thus observed. Despite the care and the time taken during the experiments, the saturated packing fraction is hardly reached even after 10^6 cycles (2.8 h under 100 Hz vibrations). This leads to an ill-defined ϕ_∞ value, which seems to vary from

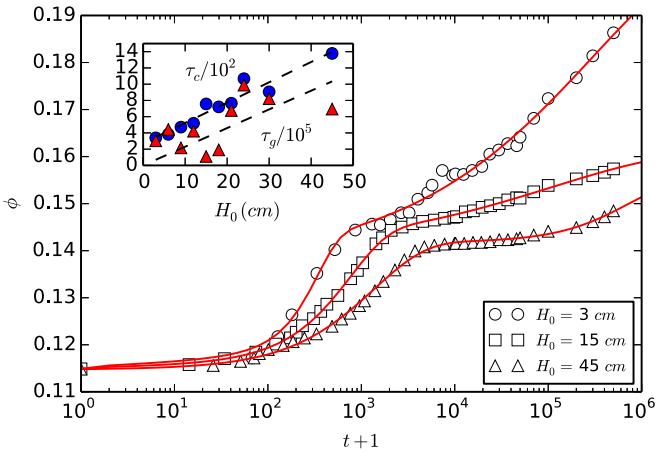

FIG. 4. Examples of experimental results for the compaction of the cohesive UO_2 powder (100 Hz, $7g$) in a 15×15 mm^2 square section tank. Data are fitted by Eq. (9). Inset: Characteristic times τ_c (solid blue circles) and τ_g (solid red triangles) as a function of the initial height H_0.

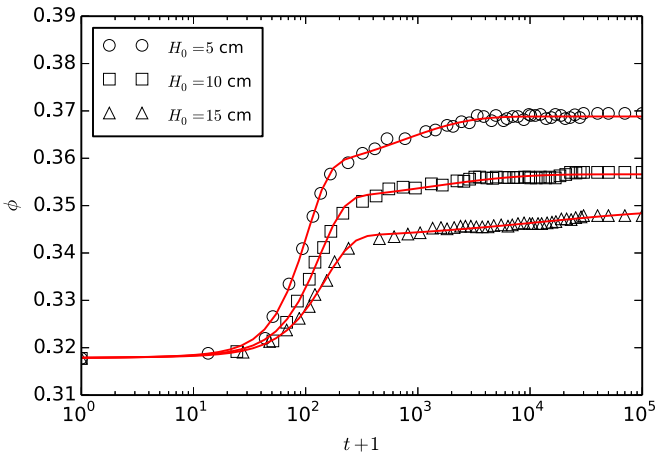

FIG. 5. Experimental results for the compaction of the weakly cohesive alumina powder (100 Hz, $7g$) in a 15×15 mm^2 square section tank. Data are fitted by Eq. (9).

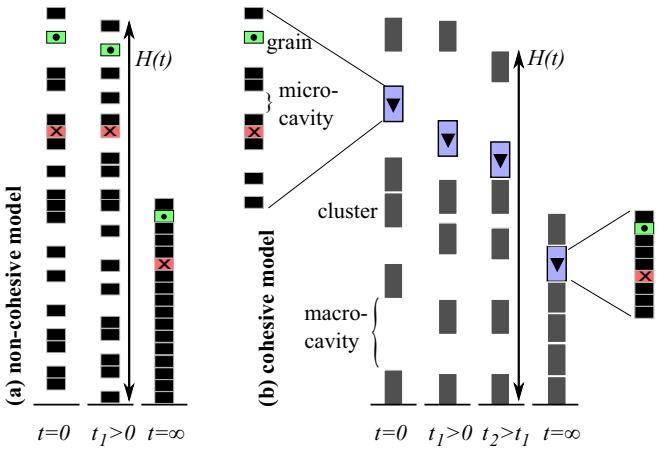

FIG. 6. (a) Sketch of the noncohesive model with individual grains only. From $t = 0$ to t_1, the dot-labeled grain (green) is allowed to move downwards whereas the cross-labeled grain (red) cannot move. (b) Sketch of the cohesive model with six clusters containing nine grains each. The triangle-labeled cluster (blue) may move down a distance of its size (from $t = 0$ to t_1) or of the available space (from t_1 to t_2).

one experiment to another. This may be caused by the filling procedure of a very cohesive powder in a constrained tank, leading to an inhomogeneous and random initial configuration. However, it is clear that at least two time scales are involved in this compaction process. Note that the very low packing fraction of this powder (in the range 0.1–0.2) is due to the large internal porosity of the UO_2 grains.

Another cohesive powder was tested with the same experimental setup and method. We used a polydisperse alumina powder (BA15W powder provided by Baikowsky) with a mean grain diameter of 90 μm, and a Hausner ratio $I_H = 1.12$. The results of the compaction are shown in Fig. 5 for a 100 Hz and $7g$ vibration. With a weaker cohesion property, the second stage of compaction seems to be present but is less remarkable than for the UO_2 powder. This is coherent with the low I_H value. In the following, we will then focus on the UO_2 powder results to understand the role of cohesion in the compaction process.

III. STOCHASTIC MODEL

To understand these results, we propose a stochastic model based on the following assumptions. When an external mechanical pulse (either a vertical tap or a horizontal vibration) is applied to a packing of granular material, there is a probability that the contacts surrounding an individual grain are broken. Hence this grain may move, explore its surroundings, and very probably move down if a void is available. When cohesion is taken into account, some grains may stay linked together and hence present a collective motion as a cluster. If the cohesion is strong enough, a cluster of grains may behave as an individual grain of a larger size. We detail below the algorithms and results obtained for two systems: a noncohesive material, and a cohesive material.

A. Compaction of a noncohesive granular material

For a noncohesive granular system, the model is a set of N unit grains shared out on a discretized one-dimensional space of size H_0 bounded with a static grain at the bottom $z = 0$ [see Fig. 6(a)]. The initial linear fraction is $\phi_{0g} = N/H_0$ and we write $\phi_{\infty g} = 1$ as the maximum packing fraction. The free spaces between two consecutive grains model the pore space between physical grains and are of the same order of magnitude as the grain volume [11].

At each time step, all the grains are tested in a random order. For each grain a random number r determines its ability to move: If $r \leq p_g$, it may move down a space unit only if the space below is free. The grain motion probability p_g is governed by the packing fraction as

$$p_g(\phi_g) = \frac{\phi_{\infty g} - \phi_g(t)}{\phi_{\infty g} - \phi_{0g}}, \tag{3}$$

which is the ratio of the free volume [12] at time t by the free volume at time $t = 0$. Many other expressions of this probability (also named mobility) available in the literature [12,13] are derived from statistical physics principles, but we prefer an expression which expresses a decrease of this probability from the initial state (ϕ_{0g}) to the final state ($\phi_{g\infty}$) in the simplest way.

We checked that the order of tests of the N grains had no influence on the global dynamics. At the end of the loop on the N grains, the global packing fraction $\phi(t) = N/H(t)$ is simply computed with the height $H(t)$ of the highest grain of the set at time step t. The computation stops after a predefined number of time steps. The system obviously no longer evolves when the packing fraction has reached its maximum limit $\phi_{\infty g} = 1$. To avoid random fluctuations on the results, several runs were averaged before presenting the results.

A representative evolution of the stochastic model is shown in Fig. 7, with a monotonous increase of ϕ from the initial value ϕ_{0g} to the limit value $\phi_\infty = 1$, the maximum packing fraction. While the numerical data are well fitted by the exponential relaxation equation (2), the inverse logarithmic law [Eq. (1)] fails to represent our data. In this log-linear plot, an inflexion point at $t = T$ may be characterized from the second derivative

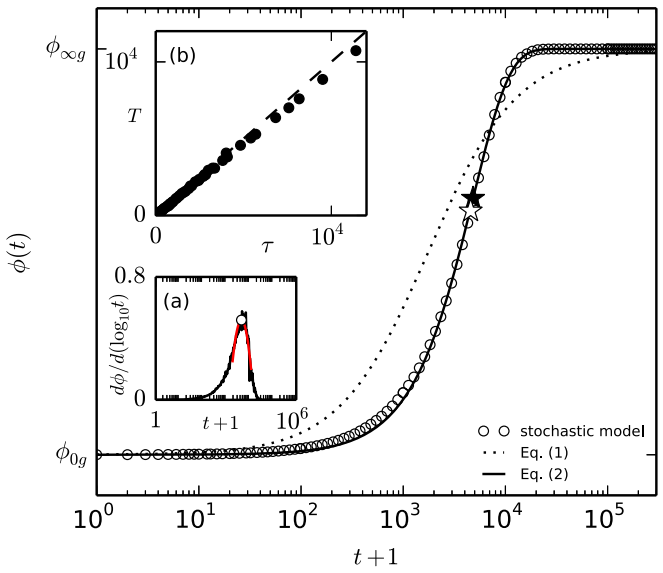

FIG. 7. A representative evolution of the packing fraction for a noncohesive granular system. $N = 3000$, $\phi_{0g} = 0.5$, $\phi_{\infty g} = 1$, data are averaged on five runs. The black star highlights the characteristic time $\tau = 4826$ used in Eq. (2) with $\beta = 1.2$, while the white star shows the characteristic time $T = 4569$ defined by Eq. (4). Inset (a): Derivative $d\phi/d[\log_{10}(t+1)]$ and its fitting by a parabola (red line) to find the characteristic time T (white dot). Inset (b): T vs τ with a unit slope (dashed line).

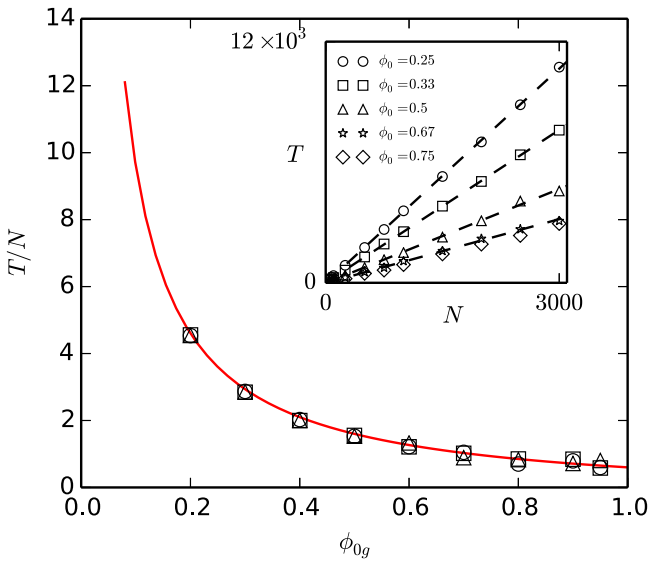

FIG. 8. The characteristic time T as a function of ϕ_0 for various numbers of grains: $N = 500$ (○), $N = 1000$ (□), $N = 1500$ (△). The continuous red curve is Eq. (5). The inset shows the linear dependence of T on N, for various initial packing fractions (see the legend).

of ϕ relatively to $\log_{10}(t+1)$,

$$\left(\frac{d^2\phi}{d[\log_{10}(t+1)]^2}\right)_{t=T} = 0. \tag{4}$$

The red star symbol in Fig. 7 thus indicates the characteristic time T of compaction, analogous to the τ parameter of the stretched exponential *ad hoc* function (indicated by a black star in the figure).

From this stochastic model, the characteristic time T varies linearly with the number of grains, but also depends on the initial packing fraction, as shown in Fig. 8 for various initial densities and grain numbers N. This result is in contradiction with Hao's analysis [14,15], where τ is said to be the inverse of the mass of powder submitted to vibration. The characteristic time of compaction is well represented by

$$T = N\left(\frac{\phi_{\infty g} - \phi_{0g}}{\phi_{0g}} + A\right), \quad \phi_{0g} < \phi_{\infty g}, \tag{5}$$

with a fitting parameter $A = 0.6$.

Since τ and T are very close, in the following, and despite the stretched exponential function lacking a full physical meaning for granular compaction, we will only refer to Eq. (2) to depict the compaction evolution for both the stochastic model and experiments.

While the experimental data from a 3D experiment are also well fitted by Eq. (2), a comparison with the one-dimensional (1D) stochastic model is difficult since the final packing fraction in the experiment clearly depends on the beads' mass in the tank. Indeed, the experimental final packing fraction ϕ_∞ decreases when the beads' mass increases. However, plotting τ/H_0 vs ϕ_∞/ϕ_0 (inset in Fig. 1) shows a linear trend, and this seems to validate Eq. (5), with the underlying assumption that the number of grains N in the experiment is proportional to H_0 or to the quantity of beads (Fig. 1). The compaction characteristic time is thus proportional to the number of movable objects. With a large assembly of grains, this time is often very large, and is then difficult to reach with a short-time experiment.

B. Compaction of a cohesive granular material

The previous stochastic model may be extended to simulate the vibration-induced compaction of a cohesive granular system with the following assumptions: The cohesive granular system is modeled as a set of N unit grains shared out between N_c clusters, with each cluster containing n grains. In the present model, the grains are not allowed to detach or attach to a cluster, as in the model developed by McCoy and Madras [16]. The parameter n is thus a fixed parameter of the stochastic model and represents the magnitude of the cohesion force between neighboring grains. As previously, the grains and clusters are located on a discretized one-dimensional space of size H_0 bounded with a static grain at the bottom $z = 0$. The initial state is prepared first by randomly placing clusters of even size n/ϕ_{0g} without an overlap, with a linear fraction of clusters ϕ_{0c}. Then the grains are randomly placed inside each cluster with a linear fraction ϕ_{0g}. The initial global packing fraction is then $\phi_0 = \phi_{0c}\phi_{0g}$. These assumptions are based on the observations described previously (Fig. 3), which suggest that at least two scales of porosity exist in the cohesive material: a small-scale porosity between neighboring grains, and a large-scale porosity induced by the formation of vaults and bulk holes.

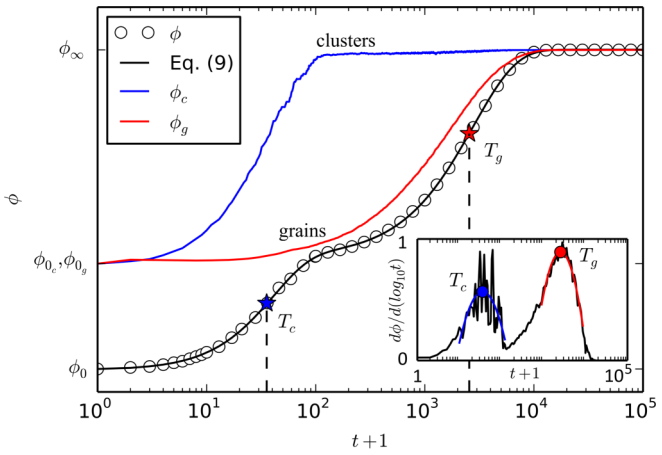

FIG. 9. Evolution of the packing fraction for a cohesive granular system of $N = 1250$ grains shared out in $N_c = 25$ clusters for $\phi_{0c} = \phi_{0g} = 0.5$ and $\phi_\infty = 1$. Data are averaged on ten runs. The stars indicate the two characteristic times T_c (blue star) and T_g (red star). The inset shows the derivative $d\phi/d[\log_{10}(t+1)]$ and its fitting by two parabolas to find the two characteristic times T_c (left blue dot) and T_g (right red dot).

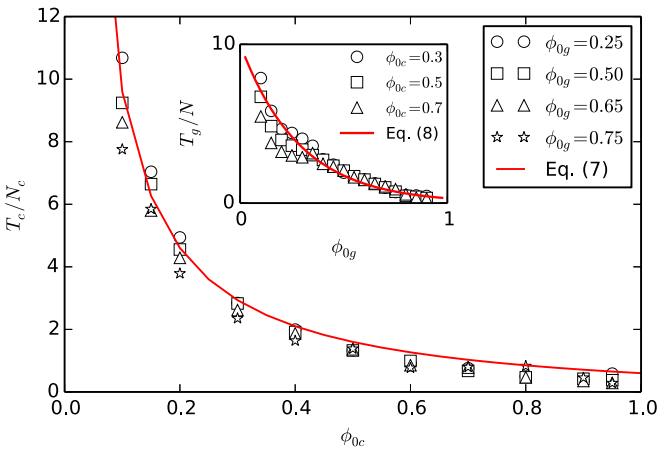

FIG. 10. Characteristic time for the cluster compaction T_c as a function of the initial cluster fraction ϕ_{0c}. Inset: Characteristic time for the grains T_g as a function of the initial intercluster grain fraction ϕ_{0g}.

At each time step, the particles and the clusters may move according to the motion probability laws

$$p_c(\phi_c) = \frac{\phi_{\infty c} - \phi_c(t)}{\phi_{\infty c} - \phi_{0c}}, \quad p_g(\phi_g) = \frac{\phi_{\infty g} - \phi_g(t)}{\phi_{\infty g} - \phi_{0g}}, \tag{6}$$

where subscript c is for clusters, g for individual grains, $\phi_c(t)$ is the cluster linear fraction, and $\phi_g(t)$ is the linear fraction of grains inside the clusters. These probabilities are also derived from normalized free volumes (the volume difference between a packing of maximum density ϕ_∞ and a packing of density ϕ) [12]. When a cluster is allowed to move, it moves downwards with a maximum falling distance of its size. If the available space is smaller than the cluster height, the moving cluster falls down to the available space. This represents the fast collapse of macrocavities involving a large number of individual grains. The global packing fraction $\phi(t)$ is simply computed with the height $H(t)$ of the highest grain of the set: $\phi = nN_c/H(t)$. The system no longer evolves when the packing fraction has reached its limit $\phi_\infty = \phi_{\infty g}\phi_{\infty c} = 1$.

A representative result is presented in Fig. 9 where the circles plot the global particle fraction versus time in a log-linear space. It clearly shows a two-stage compaction process. The first stage ($1 < t+1 < 10^2$) is related to the compaction of clusters. It mimics the collapse of macrocavities and large voids observed experimentally in a cohesive granular system. The second stage ($10^2 < t+1 < 10^5$) is related to the compaction of individual grains. Since the characteristic time of compaction is related to the number of objects (either grains or clusters), a two-stage process occurs in this model. This is confirmed by the blue and red curves on the figure showing the evolution of ϕ_c and ϕ_g, respectively.

By computing the maxima of the $d\phi/d[\log_{10}(t+1)]$ derivative, two characteristic times T_c and T_g are found (see the inset of Fig. 9). The cluster characteristic time T_c, the short-time scale, is simply transposed from Eq. (5),

$$T_c = N_c\left(\frac{\phi_{\infty c} - \phi_{0c}}{\phi_{0c}} + A\right). \tag{7}$$

This time scale does not depend on the intracluster packing fraction ϕ_{0g}, as shown in Fig. 10. The long-time scale T_g is proportional to the number of grains $N = nN_c$ and is well represented by

$$T_g = N\left[\frac{A}{2}\exp\left(\frac{\phi_{\infty g} - \phi_{0g}}{A/2}\right)\right]. \tag{8}$$

Regardless of the model parameters (ϕ_{0c}, ϕ_{0g}, N, n), the numerical results are well fitted by an extension of the stretched exponential function expression with two exponentials,

$$\phi = \phi_\infty - (\phi_p - \phi_0)e^{-(t/\tau_c)^{\beta_c}} - (\phi_\infty - \phi_p)e^{-(t/\tau_g)^{\beta_g}}, \tag{9}$$

with two time scales τ_c and τ_g, two exponents β_c and β_g, and a plateau packing fraction ϕ_p.

As for the numerical results, the experimental data from the cohesive powders are well fitted by (9), as shown by the red curves in Figs. 4 and 5. The experiments have been performed for various initial heights H_0 of the cohesive powder, and for each experiment we calculated the fitting parameters. We show that both τ_c and τ_g increase linearly with H_0 (inset in Fig. 4), which is in agreement with the stochastic model, within the assumption that $nN_c \propto H_0$. Because of a lower I_H number for the alumina powder, the influence of the powder height on the characteristic times could not be put in evidence as clearly as in the UO_2 powder. Despite some experimental uncertainties, these two well-separated time scales may be related by small and large moving objects in the experiment, grains and clusters, respectively.

IV. CONCLUSIONS

With this simple stochastic model, the packing evolution of a cohesive granular material is modeled as a set of clustered grains with two kinds of time-step motions: a collective motion linked to clusters, and an individual motion linked to individual

grains. This model allows one to represent the compaction of noncohesive or cohesive granular materials and leads to a better understanding of the characteristic time scales of the compaction. The comparison between our model and some experimental results is made through stretched exponential fitting functions (2) and (9). One of the main results of our study is that the compaction characteristic time is related to the number of objects (clusters or grains) which have to be moved during the process. For the two cohesive powders used in the experiments, a double exponential fitting equation represents fairly well the time evolution of the packing fraction.

Such a double exponential fit has already been invoked by Barker and Mehta [17], with a short-time scale associated with individual grain motion, and a long-time scale associated with collective grain motion. But in our model, the short-time scale is linked to a collective motion of clustered particles, whereas the long-time scale is linked to a slow individual compaction of single particles.

Our results are also coherent with the recent work of Kiesgen de Richter *et al.* [18], where a two-stage compaction evolution is observed, even with a packing of monodisperse glass noncohesive beads. In that work, the first stage implies an upward compaction front with a transition from a loose to a dense packing state.

This work may be extended for multiscale structures, leading to a multiscale time evolution of the packing fraction.

[1] J. B. Knight, C. G. Fandrich, C. N. Lau, H. M. Jaeger, and S. R. Nagel, Density relaxation in a vibrated granular material, Phys. Rev. E **51**, 3957 (1995).

[2] E. R. Nowak, J. B. Knight, E. Ben-Naim, H. M. Jaeger, and S. R. Nagel, Density fluctuations in vibrated granular materials, Phys. Rev. E **57**, 1971 (1998).

[3] P. Philippe and D. Bideau, Compaction dynamics of a granular medium under vertical tapping, Europhys. Lett. **60**, 677 (2002).

[4] R. L. Carr, Evaluating flow properties of solids, Chem. Eng. **72**, 163 (1965).

[5] F. A. Gilabert, J.-N. Roux, and A. Castellanos, Computer simulation of model cohesive powders: Influence of assembling procedure and contact laws on low consolidation states, Phys. Rev. E **75**, 011303 (2007).

[6] F. A. Gilabert, J.-N. Roux, and A. Castellanos, Computer simulation of model cohesive powders: Plastic consolidation, structural changes, and elasticity under isotropic loads, Phys. Rev. E **78**, 031305 (2008).

[7] E. Azéma, F. Radjaï, B. Saint-Cyr, J.-Y. Delenne, and P. Sornay, Rheology of three-dimensional packings of aggregates: Microstructure and effects of nonconvexity, Phys. Rev. E **87**, 052205 (2013).

[8] P. Rognon, J.-N. Roux, M. Naaim, and F. Chevoir, Dense flows of cohesive granular materials, J. Fluid Mech. **596**, 21 (2008).

[9] J. E. Fiscina, G. Lumay, F. Ludewig, and N. Vandewalle, Compaction Dynamics of Wet Granular Assemblies, Phys. Rev. Lett. **105**, 048001 (2010).

[10] P. A. Gago, D. Maza, and L. A. Pugnaloni, Relevance of system size to the steady-state properties of tapped granular systems, Phys. Rev. E **91**, 032207 (2015).

[11] P. Philippe, F. Barbe, S. Bourlès, X. Thibault, and D. Bideau, Analysis by x-ray microtomography of a granular packing undergoing compaction, Phys. Rev. E **68**, 020301(R) (2003).

[12] T. Boutreux and P.-G. de Gennes, Compaction of granular mixtures: a free volume model, Physica A **244**, 59 (1997).

[13] J. J. Arenzon, Y. Levin, and M. Sellitto, Slow dynamics under gravity: a nonlinear diffusion model, Physica A **325**, 371 (2003).

[14] T. Hao, Tap density equations of granular powders based on the rate process theory and the free volume concept, Soft Matter **11**, 1554 (2015).

[15] T. Hao, Derivation of stretched exponential tap density equations of granular powders, Soft Matter **11**, 3056 (2015).

[16] B. J. McCoy and G. Madras, Cluster kinetics of density relaxation in granular materials, Phys. Rev. E **70**, 051311 (2004).

[17] G. C. Barker and A. Mehta, Transient phenomena, self-diffusion, and orientational effects in vibrated powders, Phys. Rev. E **47**, 184 (1993).

[18] S. Kiesgen de Richter, C. Hanotin, P. Marchal, S. Leclerc, F. Demeurie, and N. Louvet, Vibration-induced compaction of granular suspensions, Eur. Phys. J. E **38**, 74 (2015).